Original article

Institution of MECHANICAL ENGINEERS
Journal of PROCESS MECHANICAL ENGINEERING

Proc IMechE Part E:
J Process Mechanical Engineering
1–10

DOI: 10.1177/09544089241311351
journals.sagepub.com/home/pie
Sage

Optimizing process parameters for enhanced formability and fracture behavior in single point incremental forming of SS310 sheets

N S Balaji[1], C Sathiya Narayanan[2], C Pandivelan[3], M Sivakumar[2] and Pradeep Raja C[4]

Abstract

This research investigates the forming and fracture behavior of stainless steel 310 Grade sheets using the single point incremental forming (SPIF) process under various parameters: ball diameter, spindle speed, feed rate, and vertical step down. Employing an L9 orthogonal array suggested by Taguchi, the study evaluates formability through stress and strain-based forming limit diagrams (FLD). Structural changes were analyzed using scanning electron microscopy fractography and optical microscopy. The highest level of formability was identified at the spindle speed of 100 rpm, feed rate of 600 mm/min, ball diameter of 12 mm, and a vertical step-down of 0.3 mm. Formability analysis is given variations with a maximum of 0.931 at a wall angle of 72.71°, and minimum and medium values of 0.423 and 0.63 at all angles of 60° and 66.24°, respectively. The least and most moderate formability levels showed an 11% variation, and the least and highest formability limits had a 21% higher formability limit. The stress-based limits also increased by 10% for moderate to better formability. The findings indicate that formability increases with lower vertical step down and feed rate, as well as higher spindle speed and ball diameter. This study provides valuable insights into optimizing SPIF process parameters to enhance the quality and structural integrity of formed SS310 components.

Keywords

Sheet metal forming, SPIF, SS310, forming limit diagram, formability, microstructure, fracture analysis

Date received: 6 November 2024; accepted: 12 December 2024

Introduction

Single point incremental forming (SPIF) is one of the versatile methods of sheet metal forming, which offers relatively low cost and is highly efficient as compared to conventional forming methods in terms of tools where expensive dies are not used and thus makes it more suitable for prototype and low run production. SPIF enables localized deformation and is economical in using material in that no material is wasted. It also enables rapid changes to the design, which is well suited for continually improving and changing. Across various industries like automotive, aerospace, and medical, there is SPIF to help form micro tooling, create intricate shapes, reduce costs drastically, and increase the degree of customization. Single-point incremental forming is a practical and cost-effective method for fabricating complex structures from sheet metal.[1] Widely utilized in industries, incremental sheet metal forming and employing CNC machines are economical to fabricate prototypes. Notably, the single-point and two-point incremental forming processes have emerged as successful methods.[2] Traditionally, the SPIF process employs three-axis CNC milling machines, utilizing forming tools composed of hardened carbon steel with diameters ranging from 8 to 10 mm, typically spherical or ball-ended in shape. Despite its utility, SPIF presents several drawbacks, including sheet material springback, low precision, orange peel effect, pillow effect, and low production rates[3–5] In strain analysis within sheet metal forming processes, square and circular grid techniques are prevalent. Strain measurement often

[1]Department of Mechanical Engineering, SRM Institute of Science and Technology, Tiruchirappalli, Tamil Nadu, India
[2]Department of Production Engineering, National Institute of Technology, Tiruchirappalli, Tamil Nadu, India
[3] Manufacturing Division, School of Mechanical and Building Sciences, VIT University, Vellore, Tamil Nadu, India
[4]School of Marine Engineering and Technology, Indian Maritime University, Kolkata, India

Corresponding author:
N S Balaji, Department of Mechanical Engineering, SRM Institute of Science and Technology, Tiruchirappalli Campus, Tiruchirappalli, Tamil Nadu, 621 105, India.
Email: nsbalajicad@gmail.com

relies on deformed grid images captured by USB microscopes, analyzed through ellipse fitting algorithms, segmentation approaches, least square methods, and arc support line methods.[6] SPIF represents a cutting-edge advancement in sheet metal forming technology within modern manufacturing, particularly for shaping various sheet metal configurations like cups, cones, and straight grooves with variable wall angles. Notably, these die-less forming processes offer cost-effective solutions ideal for small-batch production, increasingly finding applications in aerospace and automotive industries.[7,8] The demand for formed sheet metal components is critical in transportation and aerospace applications, with SPIF proving advantageous for both prototype and final product stage testing.[9] SPIF's customization potential to match human body shapes is invaluable, particularly in medical implant applications. Specific applications include knee prostheses, palate prostheses, ankle supports, cranial plates, facial implants, and backseat prostheses.[10] Researchers like Ham et al.[11] and Durante et al.[12] have provided insights into SPIF process parameters and effects on various materials, while Narayanaswamy et al.[13,14] and Do et al.[15] have explored formability behaviors and compared experimental and theoretical findings. Moreover, various researchers have investigated the SPIF process using both experimental approaches and theoretical models. Their studies have emphasized the significant impact of process parameters on formability, with particular attention to material types and thicknesses.[16,17] The L9 orthogonal array is a common experimental design technique developed from Taguchi robust design method, which is used in single point incremental forming process for making efficient changes in the process parameters. SPIF is an elastic instead of plastic-based sheet metal forming process where the material is gradually deformed with the aid of a tool following a specific path; important factors such as tool diameter, feed rate, and step depth have been discussed and noted to have a significant influence on the forming characters. An L9 array reduces experimental runs and affords easy differentiation of the individual and interaction effects, making analysis and optimization process.[18–20] Given the extensive literature, This research aims to study the mechanical response of stainless steel 310-grade sheets during the formability in the SPIF process based on the chosen process parameters such as ball diameter, spindle speed, feed rate, and vertical step-down. The study aims to ascertain the formability characteristics using stress and strain-based forming limit diagrams (FLDs), scanning electron microscopy (SEM) fractography, and optical microscopy. Thereby addressing a crucial gap in understanding the formability of stainless steel sheets.

Materials and methods

Materials

The stainless steel (SS310) utilized in this study was procured from a local vendor, with a standardized thickness of 0.8 mm chosen for the forming process. This thickness was deemed highly compatible with standard tools and equipment. Material element composition analysis of the SS310 sheet was conducted through spectrometry and is reported in Table 1.[21] Additionally, the microstructure of SS310 was examined using conventional metallography microscopy, as depicted in Figure 1. The optical microstructure of SS310 depicts a complete austenitic structure with an average grain size of 40 μm. The microstructures reveal various grains that are strongly and lightly etched. The grains that are in light contrast are austenitic grains whereas; the grains in dark contrast are ferrite. The austenite in SS310 exhibits FCC crystal structure and promotes excellent deformation. However, the ferrites are hard and improve the strength of the material. This contrast in morphology is attributed to the grain orientations as per Rabee and Lucke.[22]

Table 1. Material element composition of SS310.

Material element	Percentage
C	0.25
Cr	26
Mn	2
Ni	19.5
Si	1.50
S	0.03
P	0.045
Mo	0.75
Fe	Rem %

Tensile test

The tensile strength of the SS 310 material was determined following the ASTM E08 method. Tensile samples of 0°, 45°, and 90° orientations were prepared using a wire-cut EDM machine in accordance with ASTM E08 specifications.[23–25] These samples were subsequently tested using a Tinius Olsen Universal Testing Machine (UTM), as illustrated in Figure 2. The results obtained from the tensile strength tests were used to construct stress–strain curves, depicted in Figure 3.

SPIF process

The SS310 sheet blanks were prepared at dimensions of 150 mm × 150 mm for the SPIF process. These square blanks were securely fixed onto a CNC vertical milling center, where SPIF tools with ball diameters of 8 mm, 10 mm, and 12 mm were employed to conduct the incremental forming process, and these tests were performed at normal atmospheric conditions (temperature (30–34°) and humidity (80–90%)) using a CNC vertical milling machine. Various parameters of the milling center, including spindle speed, feed rate, and vertical step-down, were adjusted to achieve optimal results. Specifically, tool speeds ranged from 100 to 200 r/min, feed rates were set between 50 and 150 mm/min, and vertical movement of the tool varied from the range of

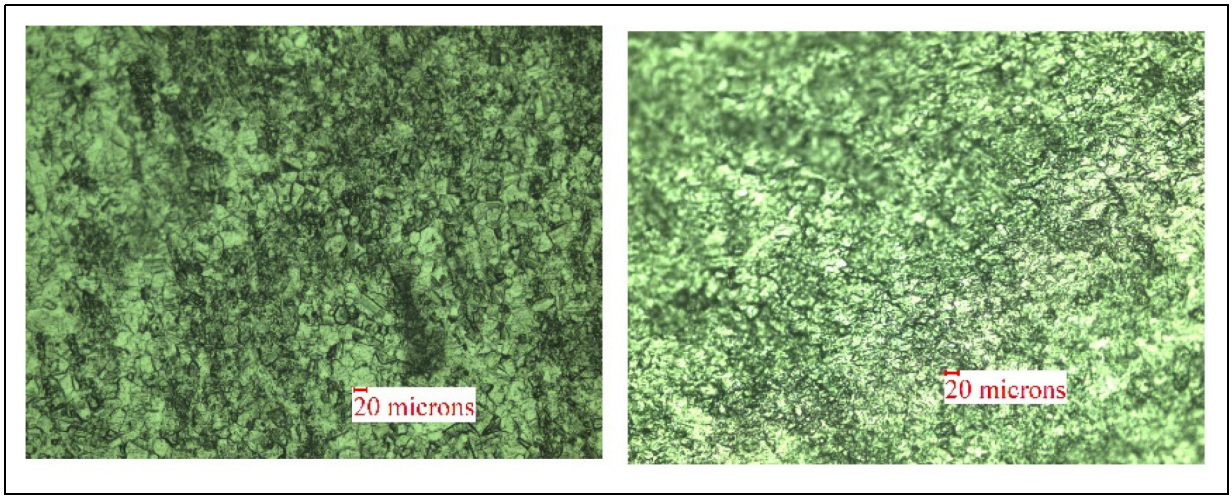

Figure 1. Microstructure of SS310.

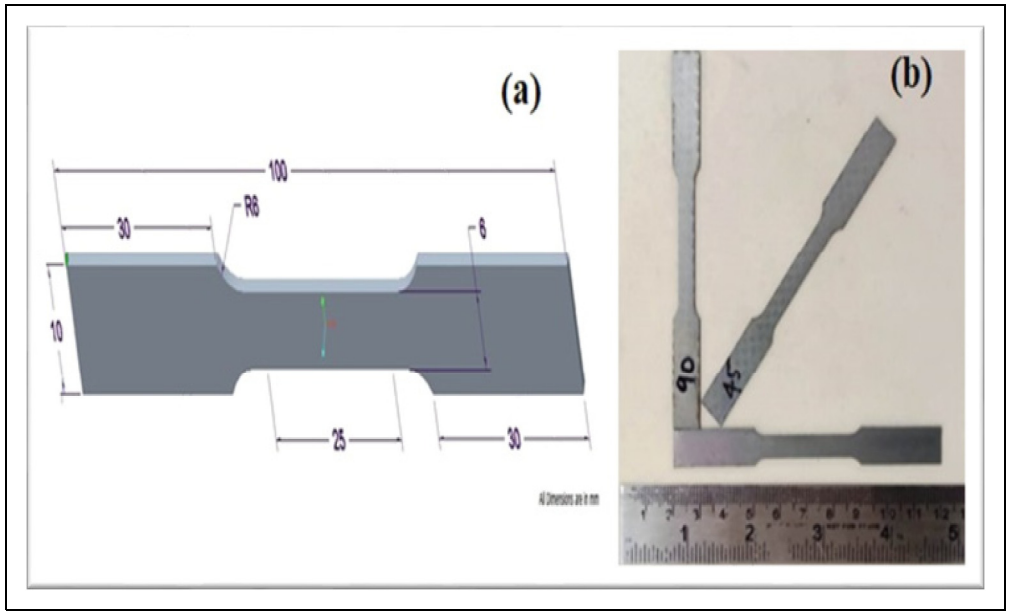

Figure 2. (a) ASTM E08 standard sample specimen, (b) tested tensile test specimens.

0.1 to 0.3 mm across three levels of uniform variations. Additionally, coconut oil was applied as a lubricant between the tool and sheets to enhance surface finish. The step-by-step procedure of the SPIF process and formed SS310 sheets are shown in Figure 4.

For FLD analysis, geometric curves were utilized to calculate deformation shapes. Prior to experimentation, small circles with reduced diameters were laser-engraved onto the SS310 flat sheets. Subsequently, the deformed shapes of these circles were utilized for strain analysis using the circle grid method. Major and minor circular diameters were measured from the formed sheets using a USB microscope, particularly focusing on areas nearest to fracture points. True strain values were then derived from these measurements, facilitating the plotting of the FLD. Furthermore, the fracture analysis during forming was observed using SEM analysis.

Result and discussion

Tensile behavior of SS310

The tensile properties of the SS310 sheet were investigated in this study in terms of load response using a UTM. From this test, properties in the following table have been acquired as shown in Table 2. It is observed that there are large differences in retrieved mechanical properties based on the orientation of the sampling plane, suggesting the anisotropy of the material. Further, the strain hardening index (n) and strength coefficient (K) were computed from the slope and intercept, respectively, of the true stress–true strain log plot (Figure 5) by equation (1). In this equation, σ represents stress, ϵ denotes strain, and K is the strength coefficient, which gives information of

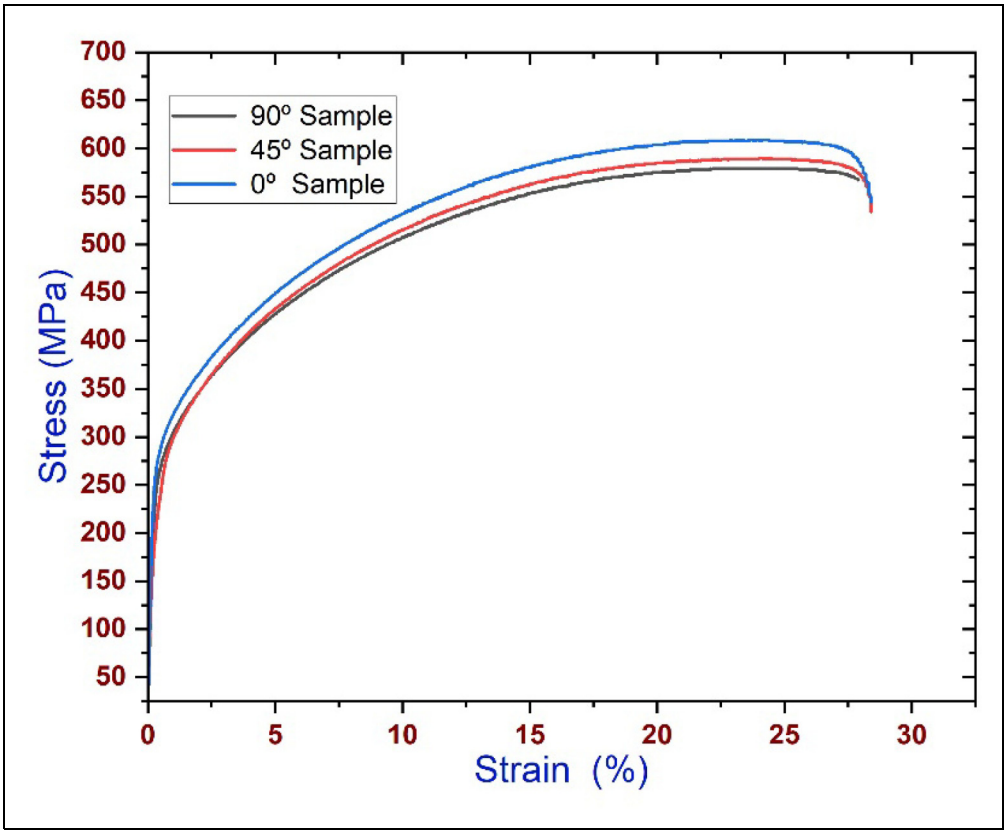

Figure 3. Engineering stress versus strain curve for SS310.

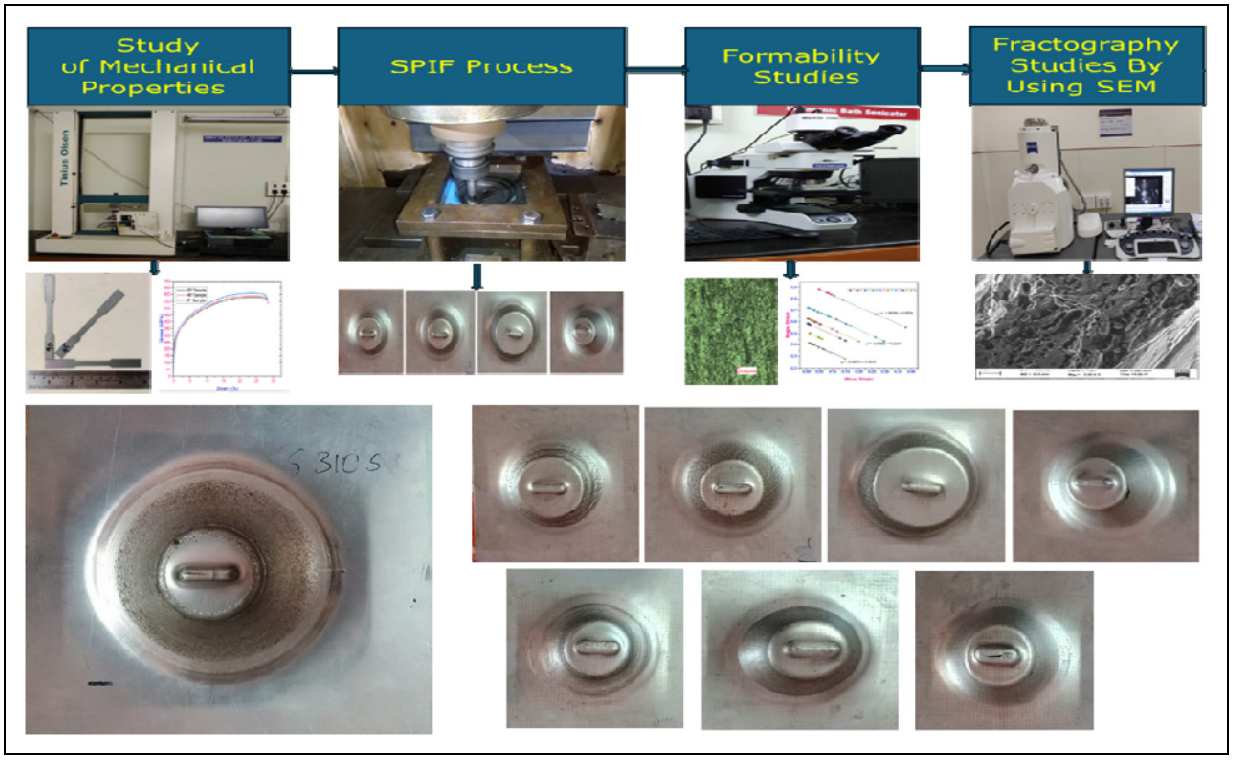

Figure 4. Step-by-step procedure of the SPIF process and formed SS310 specimen samples.
SPIF: single point incremental forming.

Table 2. Mechanical properties of SS 310.

	Mechanical properties						
Tensile sample angles	Ultimate tensile strength, (σ_u)	Yield strength, (σ_y)	% of elongation	Strain hardening exponent, (n)	Strength coefficient, (K)	Equivalent strain hardening exponent, ($\bar{n}$)	Equivalent strength coefficient ($\bar{K}$)
0°	609	281	29.2	0.2904	1170.28	0.2892	1131.62
45°	590	279	30.3	0.2901	1128.90		
90°	579	262	30.2	0.2860	1098.40		

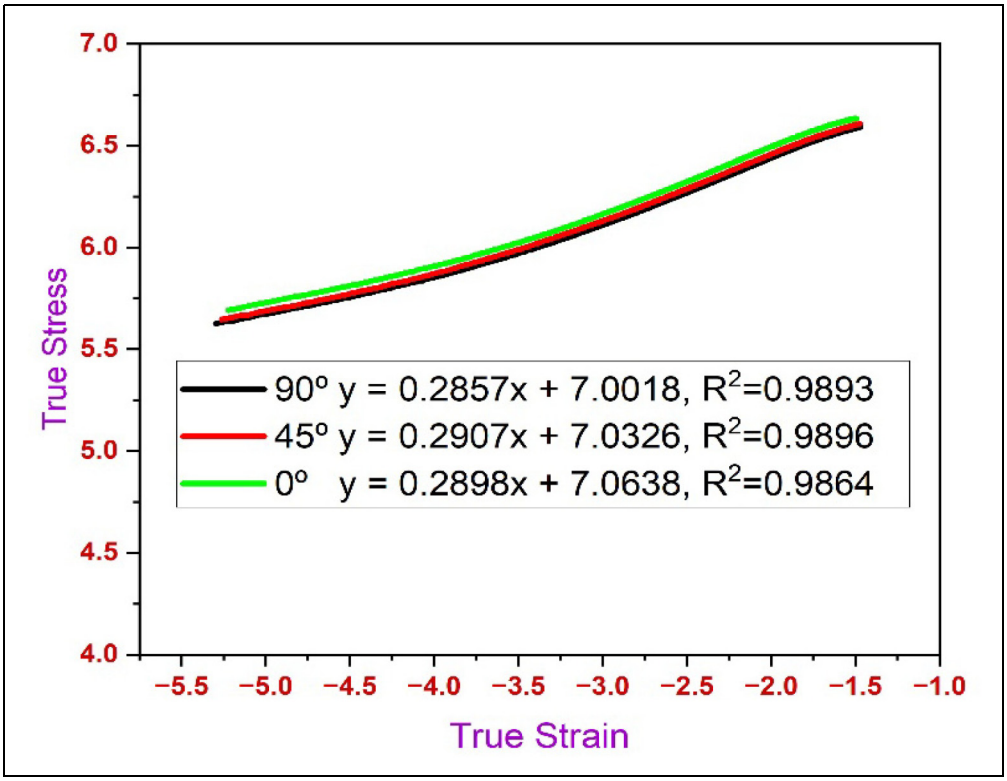

Figure 5. True stress versus true strain curve for SS310.

deformation and mechanical properties of the material quantitatively.

$$\ln \sigma = n \ln \varepsilon + \ln K \qquad (1)^{26,27}$$

At the 0° orientation, SS310 demonstrates notable ductility, with a high ultimate tensile strength (σ_u) of 609 MPa and a corresponding yield strength (σ_y) of 281 MPa. Microstructural analysis reveals a predominantly equiaxed grain structure, facilitating uniform deformation and contributing to the material's superior elongation of 29.2%.

In contrast, the 45° and 90° orientations exhibit slightly reduced mechanical properties, attributed to elongated grain structures aligned along the loading direction. Despite lower ultimate tensile strengths (σ_u) of 590 MPa and 579 MPa for the 45° and 90° orientations respectively, the materials maintain significant ductility, with elongations of 30.3% and 30.2% respectively.

The equivalent strain hardening index and strength coefficient values for the SS310 samples were calculated as 0.289 and 1131.62 respectively. These findings validate the influence of chromium content on enhancing tensile strength and imparting corrosion resistance to SS materials. The microstructure of SS310 comprises austenitic grains scattered with chromium and nickel-rich phases. Chromium-rich precipitates along grain boundaries enhance corrosion resistance, while the nickel content within the matrix improves fracture toughness by inhibiting the formation of brittle phases.[28–30]

Strain-based FLD diagram

The formability of the SS310 material was tested in a rolling direction with a straight groove test. FLD plots were generated for nine samples based on the strain values derived from various SPIF process parameters.

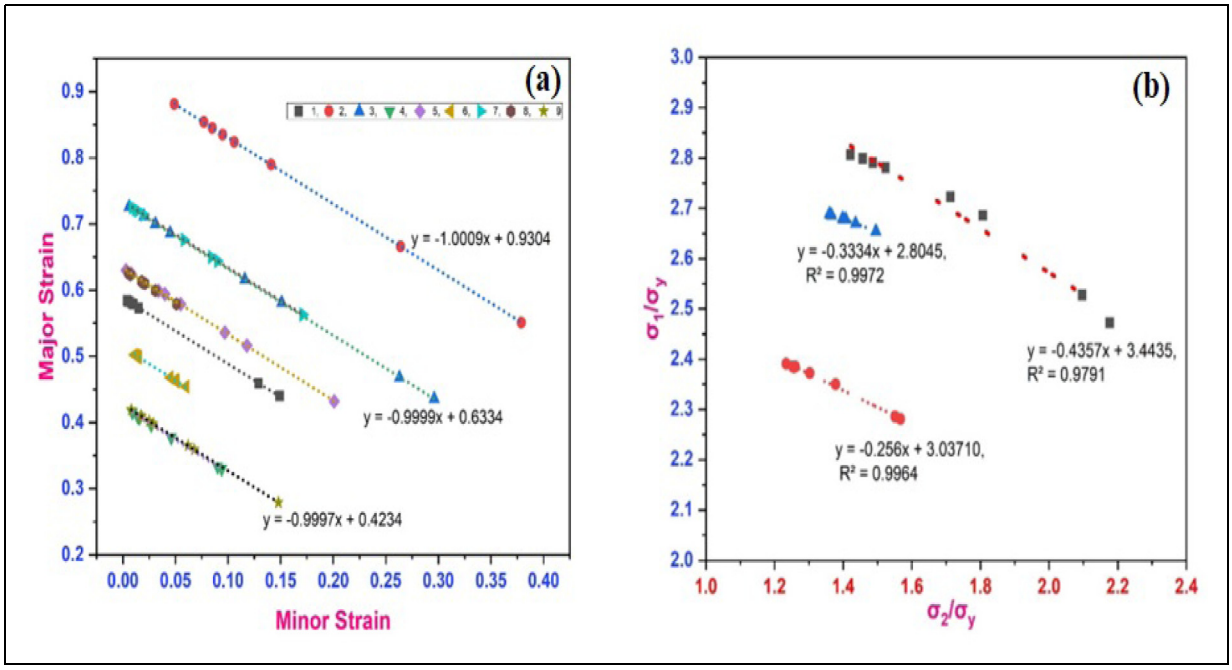

Figure 6. (a) Strain-based FLD for SS310 (b) stress-based FLD for SS310.
FLD: forming limit diagram.

The FLD curves corresponding to different process parameters are shown in Figure 6(a).

Figure 5 illustrates that the experiment yielded a minimum formability value of 0.42 under the following process parameters: 10 mm ball diameter, feed rate of 900 mm/min, spindle speed of 100 r/min, and vertical step downward movement of 0.2 mm. Intermediate formability of 0.63 was achieved with 8 mm ball diameter, feed rate of 600 mm/min, spindle speed of 200 r/min, and 0.2 mm vertical step down. Furthermore, superior formability of 0.93 was attained with 12 mm ball diameter, feed rate of 300 mm/min, spindle speed of 300 r/min, and 0.2 mm vertical step downward. Notably, the least formability resulted from a combination of medium ball diameter, lower spindle speed, moderate vertical step downward, and higher feed rate. Moderate formability values were observed when moderate spindle speed, lower ball diameter, moderate feed rate, and moderate vertical step down were combined. The highest formability values were achieved through a combination of high ball diameter, high spindle speeds, moderate vertical steps down, and low feed rates. The range of formability variation from the least to moderate was 21%, while from the least to better formability, it was 51% higher. Similarly, the transition from moderate to better formability was 30% increase in formability limits.

These results confirm that formability values are enhanced with an increased spindle speed, moderate vertical step down, and decreasing feed rate. Additionally, forming with a swiveling motion induced by spindle rotation resulted in easier sheet forming compared to straight motion. Furthermore, the influence of increasing temperature due to higher spindle speed and ball diameter, as well as strain rate, may dominate the effects of standard mechanical properties in flow and failure processes, particularly in metal forming. Overall, reducing the vertical step down and feed rate diminishes forming severity and the impact of strain hardening, ultimately enhancing formability.[31]

Stress-based FLD diagram

If a nonlinear load path is used during the forming process, the use of stress-based FLDs is strongly recommended. Stress-based FLDs are critically important when work-piece material response during multistage incremental forming, a process which uses nonlinear load paths extensively, is desired. To demonstrate the effectiveness of stress-based FLD, samples representing varying degrees of formability were selected, encompassing better, moderate, and least formability specimens, and their corresponding stress-based FLDs were plotted, as shown in Figure 6(b).

The stress-based FLDs were constructed based on the locus of normalized stress ratios. The normalization process involved dividing the principal stresses by the yield stress to obtain normalized values. For the analyzed samples, the normalized stress ratios for better, moderate, and least formability were determined to be 3.44, 3.03, and 2.80, respectively. The observed variations between the least and moderate formability were found to be 11%, while the least to better formability exhibited a significant 21% increase in formability limits. Similarly, the transition from moderate to better formability demonstrated a 10% increase in stress-based formability limits.

These findings agree with the earlier discussions, emphasizing the significant role of process parameters in aiding formability. Specifically, the results align with

the notion that increasing spindle speed, minimizing vertical step down, and augmenting feed rate significantly enhance formability. This agreement emphasizes optimizing process factors for superior formability outcomes in multistage incremental forming and similar nonlinear load path processes.

Wall angle

Table 3 highlights the relationship between ball diameter, feed rate, speed, vertical step down, formability, wall angle, and deformation. It is evident that satisfactory formability and wall angle increase with larger tool diameters, higher speeds, and decreased feed rates. This phenomenon can be attributed to the increased contact area between the work material and the tool as the diameter of the tool increases, facilitating more stretching of the material during the forming process.[32] Additionally, the absence of a necking structure prior to fracture indicates that tensile forces, which induce stretching, also contribute to crack propagation during forming.[33] The analysis indicates that stepdown has minimal impact on formability. While the formable wall angle initially increases and then decreases with incremental depth within the studied range of 0.2 mm, the variation in the formable angle remains relatively insignificant across the considered range of incremental depths. These observations emphasize the complex interaction between process parameters and formability outcomes in incremental forming processes.

Microstructural features and formability

The fractographic analysis of SS310 sheet samples with varying formability provides crucial insights into the failure mechanisms at different magnifications (2000× and 3500×). Figure 7(a) and (b), which display images of the higher formability sample, reveal the presence of dimples and intercrystalline separations indicative of ductile fracture. Prolate voids and shear dimples further confirm the material's ability to undergo significant plastic deformation before fracture. This void aspect ratio denotes the nature of the void, that is either oblate or prolate, and depending on the applied stress during the deformation/forming operation, the void transforms to prolate (elliptical in the vertical direction) or oblate (elliptical in the horizontal direction) from its initial spherical form as suggested by Gao and Kim.[34] The austenite phase of SS310 exhibits FCC crystal structure and enhances excellent formability. However, the ferrites are hard and improve the strength of the forming material.

In contrast, Figure 7(c) and (d), representing the moderate formability sample, show cleavage fractures and oblate voids. The presence of cleavage fractures suggests a combination of brittle and ductile fracture mechanisms, resulting in moderate formability. The mixed mode of failure is characterized by a combination of ductile void formation and brittle fracture propagation.

Figure 7(e) and (f), depicting the least formability sample, exhibit decohesive rupture and extensive cleavage fractures, indicating a predominantly brittle fracture mode. The oblate voids observed in the images are consistent with lower ductility and reduced formability. This brittle nature is due to higher feed rates and larger ball diameters during the incremental forming process. Optical microscopic images of samples with high, moderate, and low formability are shown in Supplemental Figure S1. These observations emphasize the complex relationship between process parameters and fracture behavior in incremental forming as stated in the above section. Lower feed rates and vertical step downs enhance ductile fracture characteristics, while higher feed rates and ball diameters promote brittle fracture mechanisms. The void area, void size, D factor, and L/W ratios, measured using AutoCAD software, provide quantifiable metrics for assessing formability. These fractographic parameters align with the overall formability trends, reinforcing the correlation between microstructural features and mechanical performance in SS310 sheets.

Void coalescence

Void coalescence in SPIF of stainless steel (SS310) is a critical aspect that requires in-depth analysis. During the SPIF process, voids can form due to various factors, such as inadequate material flow, insufficient consolidation, and localized strain concentrations. These voids

Table 3. Variation in void size (mm), void length to width ratio, d-factor, ligament thickness, and void area fraction (percent) with various spindle speeds.

Ball diameter	Feed	Speed	Vertical down	Formability	Wall angle	Deformation
8	300	100	0.1	0.427	70.29	
8	600	200	0.2	0.63	66.243	Medium
8	900	300	0.3	0.734	64.532	
10	300	200	0.3	0.513	59.71	
10	600	300	0.1	0.623	62.42	
10	900	100	0.2	0.423	60	Low
12	300	300	0.2	0.931	72.71	High
12	600	100	0.3	0.73	67.48	
12	900	200	0.1	0.598	69.338	

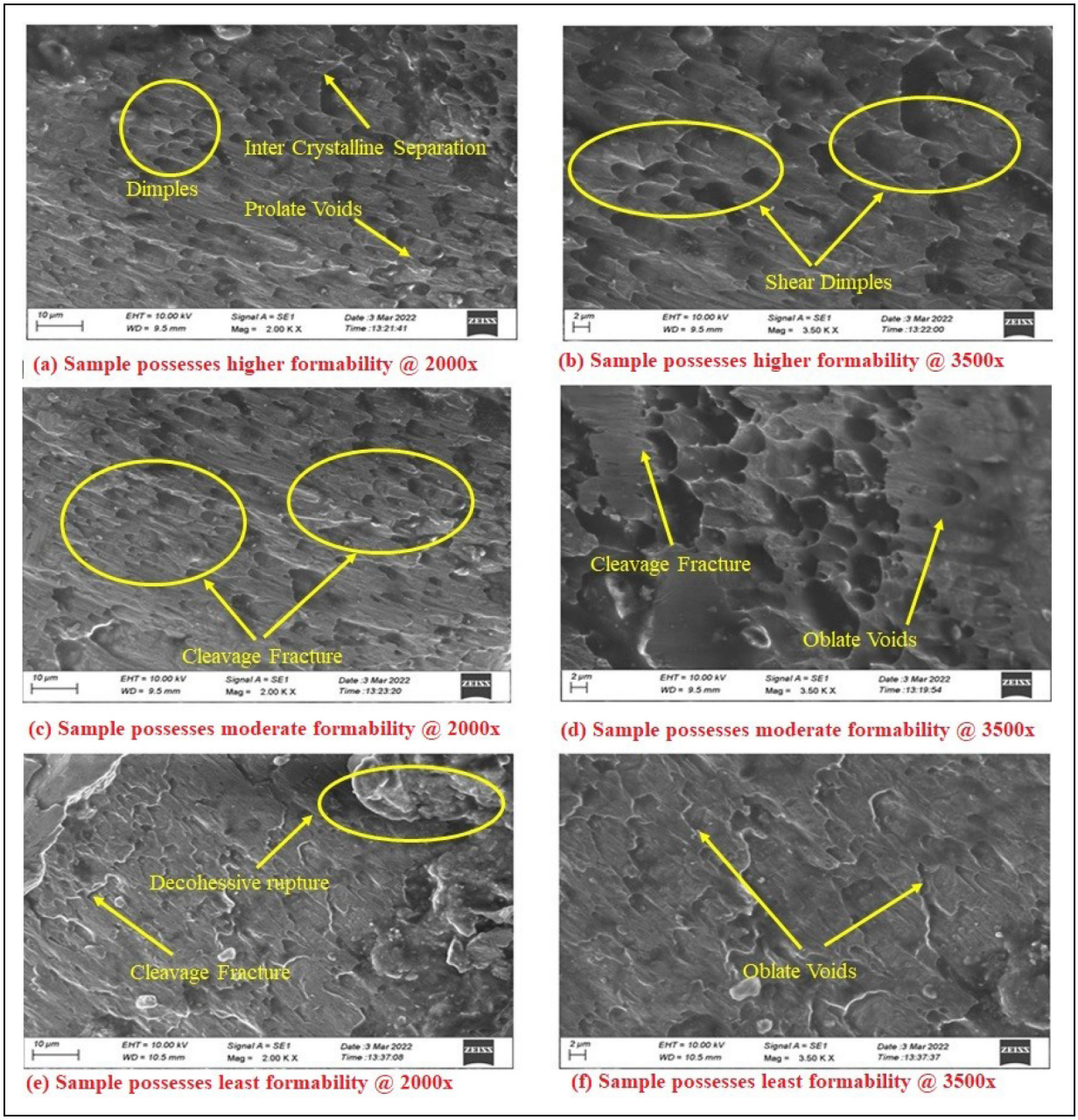

Figure 7. Fractographic analysis of SS310 sheets: correlation between microstructural features and formability.

may appear initially or develop and grow as the deformation progresses. The effective merging of these voids, known as void coalescence, is essential for achieving improved material consolidation and structural integrity.

Void coalescence is influenced by several factors, including material flow behavior, consolidation mechanisms, process parameters, and tool design. Proper material flow, characterized by significant plastic deformation and grain rearrangement, facilitates the merging of adjacent voids. Optimal process parameters, such as tool geometry, tool path, feed rate, and spindle speed need to be determined to enhance void coalescence and minimize defect formation. Additionally, the design of the forming tool plays a crucial role in promoting void coalescence. Appropriate tool shaping and sizing facilitate material flow, consolidation, and the merging of adjacent voids.[5,35–37]

The ligament thickness (LT), length-to-width (L/W) ratio, variation in the void size (mm), d factor, and void area fraction (relative) at different spindle speeds are presented in Table 3. SEM fractography of void size and void area fraction were measured and analyzed with AutoCAD software (Figure 7). Based on the deformation level, the samples were examined to study the influence of process parameters during SPIF of stainless steel 310 grade sheets. Table 3 reports the deformation levels and corresponding values obtained during SPIF.

The data obtained on deformation, D factor, ligament thickness, void size, average L/W ratio, and void area offers valuable insights into the SPIF process. The values reveal three levels of deformation: low, medium, and high, with deformation values ranging from 0.056 to 0.207. Higher deformation values indicate more

significant material deformation, suggesting increased plastic flow and thinning during forming. The D factor, ranging from 3 to 7.663, represents material thinning, with higher values indicating more substantial reduction in thickness. Ligament thickness, varying from 24.752 to 48.031, provides insights into the remaining thickness between formed features, affecting the structural integrity and strength of the components. Void size, ranging from 1.311 to 1.344, indicates the dimensions of voids present, with smaller sizes implying better material flow and consolidation. The average L/W ratio, varying between 1.311 and 1.344, reveals the aspect ratio of formed features, reflecting the extent of deformation. Finally, the void area, ranging from 0.004 to 0.126, signifies the overall area occupied by voids, which can compromise the structural integrity.[38–41]

Conclusion

This study investigates the formability characterization of stainless steel 310 grade sheets using the SPIF process with varying process parameters, focusing on structural applications. Key findings include:

1. Formability variations: The highest formability value of 0.931 was achieved with a wall angle of 72.71°, while minimum and medium formability values were 0.423 and 0.63, with wall angles of 60° and 66.24°, respectively.
2. A maximum formability of 0.931 was obtained at a wall angle of 72.71°, which is about 120% higher than the minimum formability value of 0.423 at a wall angle of 60° of the SS310 sheets. The same notion was observed with the medium formability value of 0.63, measured at a wall angle of 66.24°; this was a 49% improvement of the minimum formability value. It is clear from these results that there is significant variation in formability as wall angles are raised further, therefore calling for more effort to be put into decreasing wall angles to improve material performance.
3. Stress-based formability: Stress-based formability results showed an 11% variation between the least and moderate formability, and a 21% higher formability limit between the least and better formability. The moderate to better formability exhibited a 10% increase in stress-based limits.
4. Ductile and brittle fractures: Higher ductility conditions resulted in higher formability, while brittle conditions yielded lower formability. Low feed rate and vertical step down enhanced ductile fracture nature, while higher ball diameter and feed rate promoted brittle fracture.
5. Step down effect: The study concluded that step down has minimal effect on formability, with minor variations in the formable wall angle within the considered range of incremental depths.
6. Void analysis: Void area variations provide insights for optimizing SPIF process parameters to minimize void formation, control deformation, and enhance component quality. The void area fraction increases with higher spindle speeds.

These findings clarify the complex relationship between SPIF process parameters and formability, offering valuable guidance for optimizing manufacturing processes to improve material performance and structural integrity.

Declaration of conflicting interests

The authors declared no potential conflicts of interest with respect to the research, authorship, and/or publication of this article.

Funding

The authors received no financial support for the research, authorship, and/or publication of this article.

ORCID iDs

N S Balaji https://orcid.org/0000-0002-7178-5613
C Sathiya Narayanan https://orcid.org/0000-0001-8271-5912

Supplemental material

Supplemental material for this article is available online.

References

1. Jeswiet J, Micari F, Hirt G, et al. Asymmetric single point incremental forming of sheet metal. *CIRP Ann* 2005; 54: 88–114.
2. Liu Z, Li Y and Meehan PA. Vertical wall formation and material flow control for incremental sheet forming by revisiting multistage deformation path strategies. *Mater Manuf Processes* 2013; 28: 562–571.
3. Raju C and Narayanan CS. Application of a hybrid optimization technique in a multiple sheet single point incremental forming process. *Measurement (Mahwah N J)* 2016; 78: 296–308.
4. Shrivastava P and Tandon P. Investigation of macro-and grain-scale residual stresses with an emphasis on springback behavior in preheated incrementally formed AA 1050 H14 components. *J Mater Eng Perform* 2024; 33: 7518–7527.
5. Choudhary S and Mulay A. Influence of tool size and step depth on the formability behavior of AA1050, AA6061-T6, and AA7075-T6 by single-point incremental forming process. *J Mater Eng Perform* 2024; 33: 3283–3298.
6. Wankhede P, Kodey S, Kurra S, et al. A low cost surface strain measurement system using image processing for sheet metal forming applications. *Measurement (Mahwah N J)* 2022; 187: 110273.
7. Jie L, Jianhua M and Shuhuai H. Sheet metal dieless forming and its tool path generation based on STL files. *Int J Adv Manuf Technol* 2004; 23: 696–699.
8. Amino M, Mizoguchi M, Terauchi Y, et al. Current status of 'dieless' amino's incremental forming. *Procedia Eng* 2014; 81: 54–62.
9. Behera AK, de Sousa RA, Ingarao G, et al. Single point incremental forming: an assessment of the progress and

technology trends from 2005 to 2015. *J Manuf Process* 2017; 27: 37–62.
10. Centeno G, et al. Recent approaches for the manufacturing of polymeric cranial prostheses by incremental sheet forming. *Procedia Eng* 2017; 183: 180–187.
11. Ham M and Jeswiet J. Single point incremental forming and the forming criteria for AA3003. *CIRP Annals* 2006; 55: 241–244.
12. Durante M, Formisano A and Lambiase F. Formability of polycarbonate sheets in single-point incremental forming. *Int J Adv Manuf Technol* 2019; 102: 2049–2062.
13. Narayanasamy R and Narayanan CS. Forming, fracture and wrinkling limit diagram for if steel sheets of different thickness. *Mater Des* 2008; 29: 1467–1475.
14. Narayanasamy R and Sathiya Narayanan C. Some aspects on fracture limit diagram developed for different steel sheets. *Mater Sci Eng A* 2006; 417: 197–224.
15. Do VC, Pham QT and Kim YS. Identification of forming limit curve at fracture in incremental sheet forming. *Int J Adv Manuf Technol* 2017; 92: 4445–4455.
16. Teja PJ, Shubham R, Jain R, et al. SPIF of micro-FSWed dissimilar AlMgSi alloy: formability analysis. *Mater Manuf Processes* 2024; 39: 597–609.
17. Al-Sabur R, Kubit A, Khalaf HI, et al. Analysis of surface texture and roughness in composites stiffening ribs formed by SPIF process. *Materials (Basel)* 2023; 16: 2901.
18. Pandre S, Kumar GP, Kotkunde N, et al. Analysis of forming characteristics for dual phase steel under warm incremental forming process. *Proce of the Instit of Mech Eng, E: J of Process Mech Eng* 2024; 238: 511–519.
19. Dutta BJ and Chandna P. Process variables optimization for multiple responses in SPIF of titanium using Taguchi-GRA. *Eng Res Exp* 2023; 6: 015004.
20. Ismail NA, Ismail MIS, Radzman MAM, et al. Parametric optimization of robot-based single point incremental forming using Taguchi method. *Int J of Integr Engg* 2019; 11: 269–275.
21. Hannan A, Mehmood S, Ali MA, et al. Machining performance, economic and environmental analyses and multi-criteria optimization of electric discharge machining for SS310 alloy. *Sci Rep* 2024; 14: 28930.
22. Raabe D and Lücke K. Influence of particles on recrystallization textures of ferritic stainless steels. *Steel Res* 1992; 63: 457–464.
23. Ahamed J, Chinnaiyan FA, Vashishta P, et al. Hydroforming of nimonic 80 A sheet: a novel optimization based numerical simulation. *Int J on Interact Des Manuf (IJIDeM)* 2024: 1–13.
24. Mohan A., Uppara R. B., Jagadeesh P., et al. Formability characteristics of Al 8011 alloy sheets. In: *Advanced materials in engineering applications*. London: CRC Press, 2024, pp. 1–10.
25. Reddy MS, Singaravelu DL and Narayanan CS. Incremental sheet forming of duplex stainless steel; effect of microstructure and texture evolution on tensile behavior. *J of The Instit of Eng (India): Series D* 2024: 1–10.
26. Sathiyaseelan S, Kalimuthu R, Sathiya Narayanan C, et al. Single-point incremental formability of Monel 400: coupled grey relational and principal component analyses. *Proce of the Instit of Mech Eng, E: J of Process Mech Eng* 2024: 09544089241288936.
27. Alhomidan AA. Influence of spindle speeds on the formability, microstructure, mechanical properties and fracture behaviour of Ti-6Al-4 V alloy foils during single point micro incremental forming (SPMIF) process. *IntJ Mater Form* 2024; 17: 50.
28. Chandra Sekhar K, Narayanasamy R and Venkateswarlu K. Formability, fracture and void coalescence analysis of a cryorolled Al-Mg-Si alloy. *Mater Des* 2014; 57: 351–359.
29. Krishna K, Vigneshwaran S, Chandra Shekar K, et al. Mechanical behavior and void coalescence analysis of cryorolled AA8090 alloy. *Int J of Adv Manuf Technol* 2017; 93: 253–259.
30. Bhattacharya A, Maneesh K, Reddy NV, et al. Formability and surface finish studies in single point incremental forming. *J Manuf Sci Eng* 2011; 133: 061020-1–061020-8.
31. Vanhulst M, Vanhove H, Carette Y, et al. Reverse rigid body motion in multi-stage single point incremental forming. *Mater Res Proce* 2022; 25: 85–92.
32. Bremen T, Bailly D, Vanhulst M, et al. Development of a collaborative online knowledge management system for incremental sheet forming. *Mater Res Proce* 2023; 25: 45–52.
33. Chang Z and Chen J. A new void coalescence mechanism during incremental sheet forming: ductile fracture modeling and experimental validation. *J Mater Process Technol* 2021; 298: 117319.
34. Gao X and Kim J. Modeling of ductile fracture: significance of void coalescence. *Int J Solids Struct* 2006; 43: 6277–6293.
35. Ramesh T, NB KB, NS B, et al. Prediction of formability and effects of process parameters on the adhesively bonded composite metallic sheets. *J Adhes Sci Technol* 2024; 38: 1378–1394.
36. Raja CP and Ramesh T. Influence of size effects and its key issues during microforming and its associated processes–a review. *Eng Sci Technol, an Int J* 2021; 24: 556–570.
37. Gulati V, Aryal A, Katyal P, et al. Process parameters optimization in single point incremental forming. *J of the Instit of Eng (India): Series C* 2016; 97: 185–193.
38. Agrawal MK, Singh P, Mishra P, et al. A brief review on the perspective of a newer incremental sheet forming technique and its usefulness. *Adv in Mater Proces Technol* 2024; 10: 506–516.
39. Ahmed AMS and Saad K. The impact of magnetic abrasive finishing (MAF) process parameters on the microhardness of stainless steel SUS420 bubble cups. *Eng Technol J* 2024; 42: 615–623.
40. Najm SM, Oleksik V and Trzepieciński T. Applications of incremental sheet forming. In *Analysis and optimization of sheet metal forming processes*. Amsterdam, Netherlands: CRC Press, 2024, pp. 128–146.
41. Darzi S, Adams MD, Roth JT, et al. Manipulating martensite transformation of SS304L during double-sided incremental forming by varying temperature and deformation path. *CIRP Ann* 2023; 72: 221–224.